Soft Matter

Soft Matter

www.rsc.org/softmatter

ROYAL SOCIETY OF CHEMISTRY

ROYAL SOCIETY OF CHEMISTRY

www.rsc.org/softmatter

Soft Matter

ARTICLE

Dual-responsive polypseudorotaxanes based on block-selected inclusion between polyethylene-*block*-poly(ethylene glycol) diblock copolymers and 1,4-diethoxypillar[5]arene

Jianzhuang Chen, Nan Li, Yongping Gao, Fugen Sun, Jianping He and Yongsheng Li*

Based on the selective recognition of the polyethylene (PE) block of polyethylene-*block*-poly(ethylene glycol) (PE-*b*-PEG) by 1,4-diethoxypillar[5]arene (DEP5A), two novel thermo and competitive guest (1,4-dibromobutane or hexanedinitrile) responsive polypseudorotaxanes (PPRs) have been successfully constructed. The formations of PPRs both in solution and in the solid state were demonstrated by ^{1}H NMR, 2D NOESY, and WAXD analyses. TGA data illustrate that PPRs exhibit higher thermal stability than their precursor diblock copolymers. Moreover, intriguing porous disk-like aggregates are produced by eletrospraying of PPRs in CHCl$_3$ and the self-assembled structures of PPRs are totaly changed by the addition of 1,4-dibromobutane or hexanedinitrile, demonstrating its competitive guest stimuli-responsiveness.

Introduction

Polyethylene (PE)-based materials play important roles in contemporary society and are widely used in many fields due to the combination of excellent physical and chemical properties along with low cost.[1] However, the lack of chemical functionality and structural diversity is the common barrier for broadening their applications.[2] Hence, it is urgent to develop the PE-based materials functionalized by polar groups or polymer segments with some improved or modified properties.

Polypseudorotaxanes (PPRs) constructed *via* host–guest complexations of covalently connected polymers with macrocycles have attracted intensive interest as new smart functional polymeric materials.[3] Due to the reversibility and responsiveness of host–guest interactions, PPRs exhibit unique topological structures and fascinating chemical/physical properties,[4] which have been used in a wide range of applications, such as self-healing polymers,[5] stimuli responsive materials,[6] molecular machines,[7] and drug delivery systems.[8] Therefore, PE-based PPRs can be considered as a new class of high-performance functional polyolefin materials, which may overcome the limitations and shortcomings of traditional PE-based materials. Though a number of PE-based block copolymers with a variety of different functions have been synthesized in recent years,[9] PE-based PPRs have been rarely reported, which can be attributed to the low solubility of PE chains in organic solvents and no polar functional groups to form complexes with macrocyclic hosts.[10]

Various classes of macrocycles, such as crown ethers,[11] cyclodextrins,[12] calixarenes,[13] cucurbiturils,[14] and pillararenes[15] have

been explored for the fabrication of PPRs. Pillar[5]arenes (P5As) are a new type of cyclophane host molecules[16] and have been widely used in constructing PPRs and other excellent supramolecular structures.[17] Recently, Huang and co-workers reported that P5As could bind *n*-hexane to form an 1:1 host–guest complex and further to form supramolecular polymers based on multiple C−H···π interactions.[18] Moreover, based on the same recognition motif, Ogoshi and co-workers synthesized PPRs from PE chains and P5As in the melt state.[10a]

It is noting that site-selective complexation plays a crucial role in constructing artificial supramolecular structures in polymeric systems[19] and block-selected PPRs constructed from PE-based block polymers and macrocycles have not been reported yet. Herein, two novel dual-responsive PE-based PPRs were successfully constructed by the selective recognition of PE block of PE-*b*-PEG by 1,4-diethoxypillar[5]arene (DEP5A). The structures and stimuli-responsive properties of PPRs were characterized by proton nuclear magnetic resonance spectra (^{1}H NMR) and two-dimensional nuclear overhauser enhancement spectroscopy (2D NOESY). The crystal properties, thermal stability, and self-assembled aggregates of PPRs were well studied by wide angle X-ray diffraction (WAXD), thermogravimetric analysis (TGA), field emission scanning electron microscope (FESEM), and transmission electron microscopy (TEM).

Experimental section

Materials

Monohydroxy-terminated PE-*b*-PEG$_{1400}$ (M_n ~ 1400 g/mol, 50 wt% of ethylene oxide, calculated molecular component is PE$_{45}$-*b*-PEG$_{39}$ from GPC and ^{1}H NMR data, see supporting information) and PE-*b*-PEG$_{2250}$ (M_n ~ 2250 g/mol, 80 wt% of ethylene oxide, calculated molecular component is PE$_{32}$-*b*-PEG$_{76}$ from GPC and ^{1}H NMR data, see supporting information) were purchased from Sigma Aldrich Corporation (St. Louis, MO). DEP5A was synthesized according to

Laboratory of Low-Dimensional Materials Chemistry, School of Materials Science and Engineering, East China University of Science and Technology, Shanghai 200237, P. R. China. E-mail: ysli@ecust.edu.cn; Fax: +86-021-6425-2599; Tel: +86-021-6425-0740
† Electronic Supplementary Information (ESI) available: [Characterization, ^{1}H NMR data and other materials]. See DOI: 10.1039/x0xx00000x

the published procedure.[16a] Chloroform ($CHCl_3$) was purchased from Sinopharm chemical reagent Co., Ltd (SCRC). All reagents were commercially available and used as supplied without further purification.

Analysis

^{1}H NMR spectra were collected on a temperature-controlled 500 MHz spectrometer with $CDCl_3$ as the solvent. GPC measurements of polymers were run at 35 ^{o}C using THF as eluent with a flow rate of 1.0 mL/min and linear polystyrene as standards. FESEM analysis was conducted on a Hitachi S-4800 electron microscope. The TEM images were obtained by a JEM-1400 Transmission Electron Microscope (JEOL Ltd, Tokyo, Japan) operated at 100 kV. WAXD measurements were carried out at room temperature using a Rigaku D/Max-2200PC X-ray diffractometer with a Cu target (40 KV, 40 mA). Powder samples were exposed at a scan rate of $2\theta = 5°\cdot min^{-1}$ between $2\theta = 5°$ and 40°. TGA was performed from room temperature to 650 °C at a heating rate of 20 °C/min under nitrogen atmosphere, using a TA Instruments Q500 series. The powder samples for WAXD and TGA analyses were prepared from precipitated PPRs in cold precipitant (methanol or diethyl ether) and dried in a vacuum oven at room temperature for 24 h. The physical blend mixtures of PE-*b*-PEGs and DEP5A in the same molar ratio of corresponding PPRs were prepared by mixing PE-*b*-PEGs and DEP5A in a mortar and pestle for 3 min.

Results and discussion

The formation of PPRs
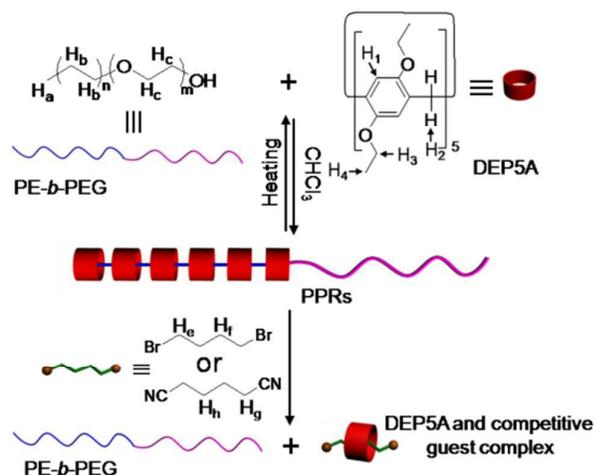
Scheme 1 Cartoon representation of the formation of PPR and its dual responsive processes.

The preparation of PPR derived from the self-assembly of PE-*b*-PEG and DEP5A in $CHCl_3$ and its dual responsive processes are presented in Scheme 1. Partial ^{1}H NMR spectra of PE-*b*-PEG$_{1400}$ upon the addition of DEP5A showed that the signals of the methylene protons at $\delta = 1.25$ ppm (H_b) in the PE block of PE-*b*-PEG$_{1400}$ shifted upfield ($\delta = 1.23, 1.21, 1.18, 1.14, 1.09, 1.06$) and splitted ($\delta = 1.04, 1.02, 0.98, 0.96$ ppm) to H_b' (accompanied with

line broadening), due to the shielding of methylene moiety by DEP5A (Fig. 1, the molar ratio of DEP5A to PE-*b*-PEG and the GPC data of PE-*b*-PEG were used to calculate). However, no shift changes were detected for the methylene protons ($\delta = 3.64$ ppm, H_c) in the PEG block. Partial ^{1}H NMR spectra of PE-*b*-PEG$_{2250}$ upon the addition of DEP5A displayed similar chemical shift changes (Fig. S5) as those of PPR1. These phenomena indicated that only the PE chains were closely encircled by the macrocyclic cavities of DEP5A, forming PPRs, whereas the PEG blocks were uncovered. From 2D NOESY NMR analysis, NOE correlation signals were observed between the methylene protons (H_b) of PE chains and the methyl (H_4) and methylene protons (H_2 and H_3) of DEP5A (Fig. S7). These observations verified that the PE segments were successfully encapsulated in the cavity of DEP5A.
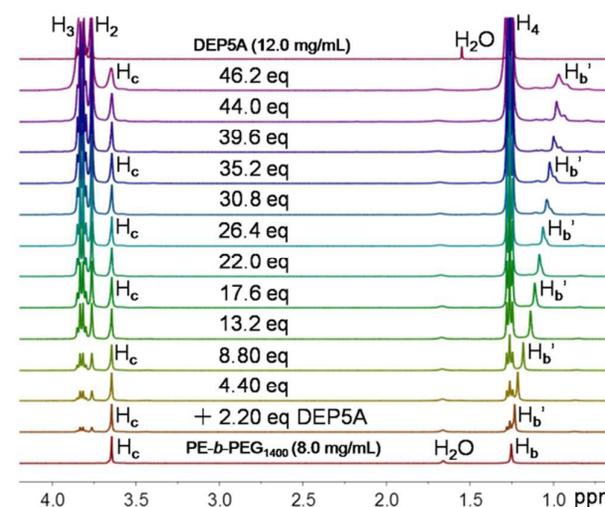

Fig. 1 Partial ^{1}H NMR spectra (500 MHz, $CDCl_3$, 20 ^{o}C) of PE-*b*-PEG$_{1400}$ upon the addition of DEP5A.

Dual-responsive processes of PPRs

Fig. 2 exhibited that the solution of PE-*b*-PEG$_{1400}$ (10.0 mg/mL) in $CDCl_3$ became transparent and turbid upon heating and cooling, respectively, showing that PE-*b*-PEG$_{1400}$ didn't dissolve well enough in $CDCl_3$ at 20 ^{o}C. With the addition of DEP5A (44.0 eq), the mixture gradually became transparent, indicating the formation of PPR1 and its higher solubility than PE-*b*-PEG$_{1400}$. With the addition of 1,4-dibromobutane (DBrBu) or hexanedinitrile (44.0 eq) to the solution, it became turbid again.[20] These revealed that the formation and deformation of PPRs could be finely tuned by adding DEP5A and DBrBu or hexanedinitrile.

Fig. 2 PE-*b*-PEG$_{1400}$ in $CDCl_3$ (10.0 mg/mL) and its tuning processes by heating and adding DEP5A or competitive guest molecule of DBrBu or hexanedinitrile.
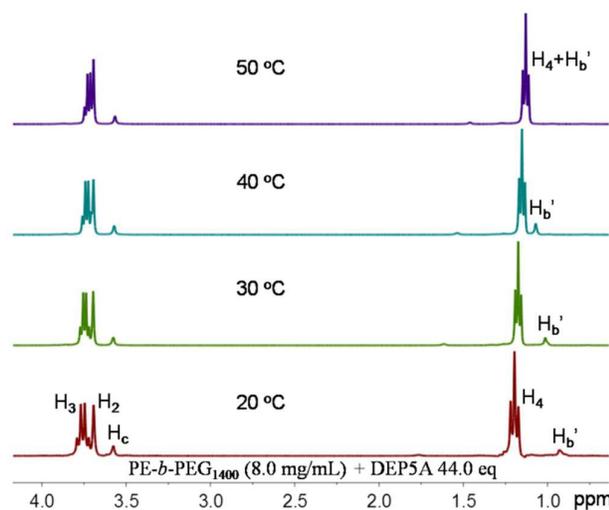
Fig. 3 Partial ^{1}H NMR spectra (500 MHz, CDCl₃) of PPR1 at different temperatures.

^{1}H NMR spectra of PPRs at different temperatures are recorded and shown in Fig. 3 and S8. At elevated temperatures, intensities of the signals at δ = 0.90–0.88 ppm shifted downfield and became slightly stronger, indicating the reversible molecular recognition between DEP5A and PE segments of PE-*b*-PEG. All these phenomena suggested that the structure of PPRs could be reversibly tuned *via* heating or cooling, exhibiting thermo stimuli-responsive.
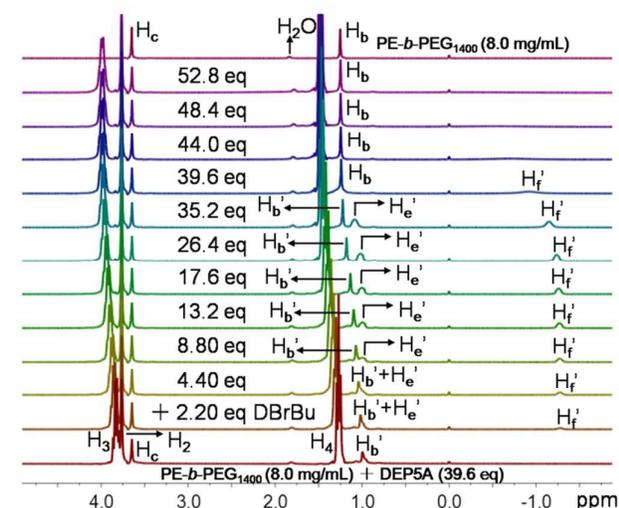

Fig. 4 Partial ^{1}H NMR spectra (500 MHz, CDCl₃, 20 °C) of PPR1 upon the addition of DBrBu.

Partial ^{1}H NMR spectra of PPR1 upon the addition of DBrBu are shown in Fig. 4. The signals of the methylene protons (δ = 1.00 ppm, H_b') in PE blocks of PE-*b*-PEG₁₄₀₀ shifted downfield (δ = 1.02, 1.04, 1.07, 1.10, 1.13, 1.18, 1.22, 1.24 ppm) to H_b (accompanied with line narrowing). DEP5A could form much stronger complex with DBrBu than with PE segments, so that the disassembly of PPR1 occurred.[20a] As the methylene moiety of PEG blocks was unshielded by DEP5A, no shifts were detected for the signals of the methylene protons (δ =

3.64 ppm, H_c) in PEG blocks of PE-*b*-PEG₁₄₀₀. In addition, as a competitive guest, the effect of hexanedinitrile on the ^{1}H NMR spectrum of PPRs was also investigated. As shown in Fig.5, the signals of methylene protons (H_b') in PE blocks of PE-*b*-PEG₁₄₀₀ shifted to H_b upon the addition of hexanedinitrile. It can be attributed to the more stable complexation between hexanedinitrile and DEP5A, making the disassembly of PPR1.[20d] There was no signal shifts detected of the methylene protons (H_c) in PEG blocks of PE-*b*-PEG₁₄₀₀ for the methylene moiety of PEG blocks was unshielded by DEP5A. Similarly, upon the addition of DBrBu or hexanedinitrile, partial ^{1}H NMR spectra of PPR2 displayed similar chemical shift changes (Fig. S12 and S16) with those of PPR1. These illustrate that the structure of PPRs could be disassembled by adding DBrBu or hexanedinitrile, exhibiting a competitive guest stimuli-responsive (Scheme 1). It can be concluded that the competitive guest which could form stable host–guest complexes with DEP5A than long alkyl chain can trigger the competitive guest stimuli-responsiveness of PPRs.
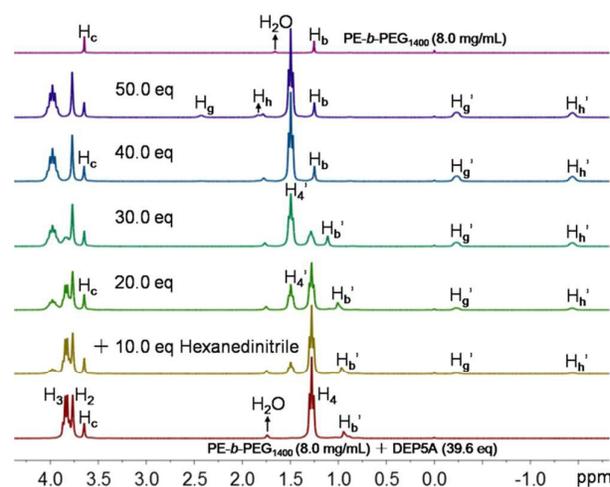

Fig. 5 Partial ^{1}H NMR spectra (500 MHz, CDCl₃, 20 °C) of PPR1 upon the addition of hexanedinitrile.

WAXD patterns of PPRs
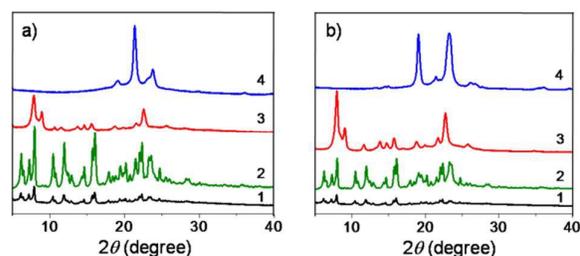
Fig. 6 WAXD patterns of DEP5A (1), physical blend mixtures of PE-*b*-PEG₁₄₀₀ and DEP5A (2), PPR1 (DEP5A 40.0 eq) (3), and PE-*b*-PEG₁₄₀₀ (4) a); DEP5A (1), physical blend mixtures of PE-*b*-PEG₂₂₅₀ and DEP5A (2), PPR2 (DEP5A 40.0 eq) (3), and PE-*b*-PEG₂₂₅₀ (4) b).

WAXD patterns of DEP5A, PE-*b*-PEG, their physical blend mixtures, and PPRs are shown in Fig. 6. It can be seen that PE-*b*-PEG₁₄₀₀ exhibits three prominent peaks at 19.2° for crystalline PEG

segments, at 21.4° for crystalline PE segments, and at 23.8° for both PE and PEG, respectively (Fig. 6a4).[10,19b] For PPR1, a number of reflection peaks are presented which are different from that of DEP5A, PE-*b*-PEG$_{1400}$, and their physical blends (Fig. 6a1,4,2). The same situation is obtained for PPR2 (Fig. 6b). These indicate that PPRs formed different crystal structures, reflecting the formation of PPRs in the solid states.
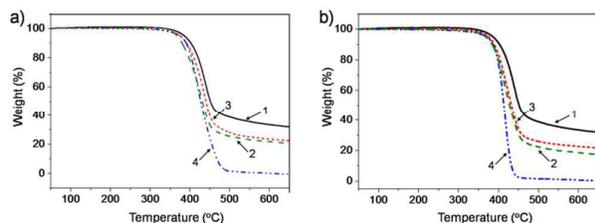
TGA of PPRs

Fig. 7 TGA scans of DEP5A (1), physical blend mixtures of PE-*b*-PEG$_{1400}$ and DEP5A (2), PPR1 (DEP5A 40.0 eq) (3), and PE-*b*-PEG$_{1400}$ (4) a); DEP5A (1), physical blend mixtures of PE-*b*-PEG$_{2250}$ and DEP5A (2), PPR2 (DEP5A 40.0 eq) (3), and PE-*b*-PEG$_{2250}$ (4) b).

The thermal stabilities of PPRs were investigated by TGA (Fig. 7). The decomposition temperature (T_d, a temperature at which 10% of mass loss has occurred) is used to evaluate the thermal stability[19a] and the results for the two PPRs are listed in Table 1. The T_d value for PPR1 is found to increase by 12 ^{o}C, and it increases by 5 ^{o}C for PPR2, as compared with their respective physical blend mixtures of PE-*b*-PEGs and DEP5A. Therefore, it is concluded that the diblock copolymers are stabilized by the formation of the PPRs, which might be attributed to the host−guest inclusion complexation between PE block of PE-*b*-PEG and DEP5A.

Table 1 Decomposition temperatures^a (T_d) of PPRs in comparison with their free components

PPRs$^{a)}$	T_d(DEP5A)$^{b)}$ [^{o}C]	T_d(PE-*b*-PEG)$^{b)}$ [^{o}C]	T_d(DEP5A/PE-*b*-PEG)$^{b)}$ [^{o}C]	T_d(PPRs)$^{c)}$ [^{o}C]
PPR1	402	391	380	392
PPR2		386	384	389

$^{a)}$ (Temperatures at which 10% of mass loss has occurred from TGA curves); $^{b)}$ (T_d for free DEP5A, free PE-*b*-PEG and their solid mixtures); $^{c)}$ (T_d for PPRs).

Self-assembly of PPRs

The size distribution curves of PPRs in CHCl$_3$ at various temperatures are shown in Fig S9 and S10. As can be seen, the particle size of either PPR1 or PPR2 increases with the temperature. It changes from 511.3 nm to 640.5 nm for PPR1 or 112.0 nm to 216.5 nm for PPR2 when the temperature was increased from 20 ^{o}C to 40 ^{o}C. This is probably due to the escaping of DEP5A from PE chain at higher temperatures, resulting in longer chain of the naked hydrophobic PE and thus the formation of large aggregate particles. Besides, it is found that the particle size of PPR2 is always smaller

than that of PPR1 at the same temperatures, as the hydrophobic PE chain of PE-*b*-PEG$_{2250}$ is shorter than that of PE-*b*-PEG$_{1400}$.

The SEM and TEM images of the aggregates of PE-*b*-PEGs, PPRs and disassembled PPRs are shown in Fig. 8. Irregular particles are observed for PE-*b*-PEG$_{1400}$ (Fig. 8a$_1$,a$_2$) and its corresponding PPR1 could self-assemble into network structures (Fig. 8b$_1$,b$_2$). When DBrBu was added to PPR1 solution, the threaded structures of PPR1 were destroyed and the square plate aggregates which may be formed by the self-assemble of the complex of DEP5A and DBrBu were visualized (Fig. 8c$_1$,c$_2$). Island shape aggregates are observed for PE-*b*-PEG$_{2250}$, (Fig. 8d$_1$,d$_2$). Its corresponding PPR2 could self-assemble into network structures which is more regular than that of PPR1 (Fig. 8e$_1$,e$_2$). This can be ascribed to the fact that PPR2 has longer soft unthreaded PEG chain and shorter rigid threaded PE chain than PPR1, making it easier to form adaptive self-assembled structures. When DBrBu was added to PPR2 solution, the square plate aggregates were also got (Fig. 8f$_1$,f$_2$). The other irregular particles beside square plate aggregates may formed by the unthreaded PE-*b*-PEG$_{2250}$. Hexanedinitrle as a competitive guest to influence the self-assembled structures of PPRs was also studied and the network structures formed by PPRs transformed into irregular aggregates after hexanedinitrle was added (Fig. S19). All these phenomena illustrated that the self-assembled structures of PPRs can be adjusted by adding competitive guest.
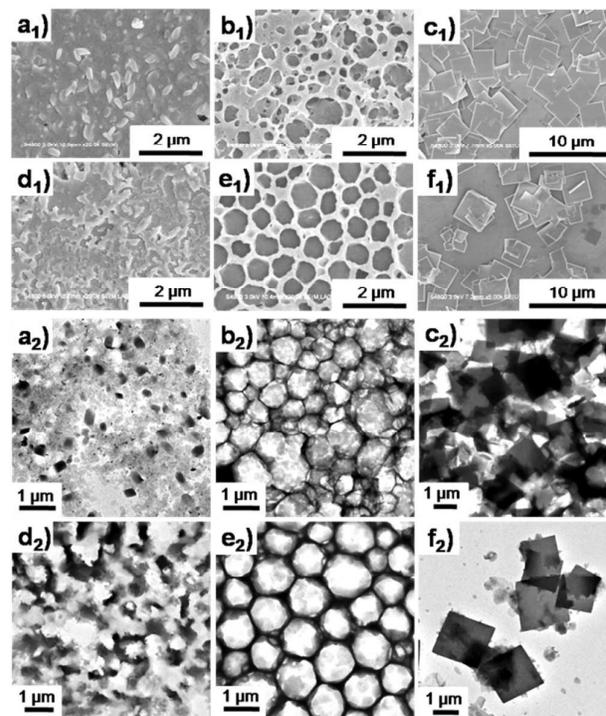

Fig. 8 SEM images of self-assembed structures in CHCl$_3$ at 20 ^{o}C: a$_1$) PE-*b*-PEG$_{1400}$ (1.0 mg/mL), b$_1$) PPR1 (DEP5A, 40.0 eq), c$_1$) 40.0 eq DBrBu was added to b$_1$); d$_1$) PE-*b*-PEG$_{2250}$ (1.0 mg/mL), e$_1$) PPR2 (DEP5A, 40.0 eq), f$_1$) 40.0 eq DBrBu was added to e). a$_2$)- f$_2$) are the TEM images of a$_1$)-f$_1$). The scale bar of a$_1$), b$_1$), d$_1$), and e$_1$) is 2 μm; The scale bar of c$_1$) and f$_1$) is 10 μm; The scale bar of a$_2$)-f$_2$) is 1 μm.

Electrospraying is a promising technology to prepare various polymer structures from solutions based on high-voltage electrostatic

ARTICLE

repulsions. The electrosprayed aggregates from $CHCl_3$ solutions of PE-*b*-PEGs and PPRs are shown in Fig. 9. Specifically, irregular aggregates (average size, 0.80 μm) and near-spherical geometry particles (average diameter, 2.60 μm) are produced from PE-*b*-PEG_{1400} and PE-*b*-PEG_{2250} solutions, respectively (Fig. 9a,d). Interestingly, dish-like aggregates (average size, 7.80 and 7.60 μm) with some pores on their surface are obtained from PPRs (Fig. 9b,e). The TEM results suggest that the core of those dish-like aggregates produced from PPRs are also porous (Fig. 9c,f). Near-spherical particles are visualized from DEP5A solution with different concentrations (Fig. S21). The regular aggregates of PPRs are totally different from those of the individual PEG-*b*-PEGs and DEP5A, further confirming the successful formation of PPRs.

Those intriguing electrosprayed porous dish-like aggregates encouraged us to explore what it was change to for disassembled PPRs. So, DBrBu was added to PPRs solution to destroy the threaded structures of PPRs. Spherical geometry particles and hemispherical aggregates with some pores on their surface were produced from disassembled PPR1 and PPR2, respectively (Fig. S22a,d). The TEM results suggested that those aggregates had less pores than these of PPRs (Fig. S22c,f). The reasons of the pores formation and the application of those tailorable aggregates of PPRs as advanced functional materials with high performance[21] are under investigation.
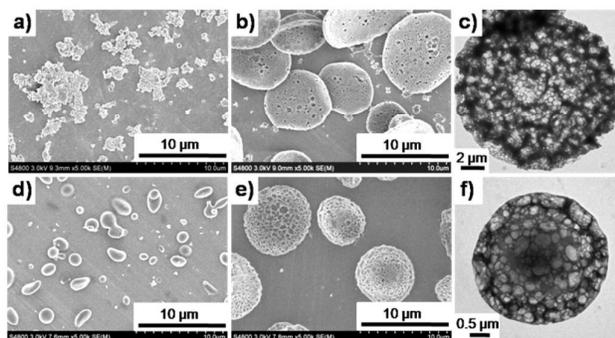

Fig. 9 FE-SEM images of electrosprayed microstructures: a) PE-*b*-PEG_{1400} 5.0 mg/mL, b) PPR1 (PE-*b*-PEG_{1400} 5.0 mg/mL, DEP5A 20.0 eq), d) PE-*b*-PEG_{2250} 5.0 mg/mL, e) PPR2 (PE-*b*-PEG_{2250} 5.0 mg/mL, DEP5A 20.0 eq). c) (scale bar: 2.0 μm) and f) (scale bar: 0.5 μm) are the TEM images of b)-e). The scale bar of a), b), d), and e) is 10 μm.

Conclusions

In summary, two novel thermo and competitive guest (DBrBu and hexanedinitrile) responsive PPRs have been successfully constructed *via* the selective recognition and threading of the PE block of PE-*b*-PEG with DEP5A efficiently. Due to their host–guest inclusion complexation, PPRs exhibit higher thermal stability than their precursor diblock copolymers. The self-assembled structures of PPRs are totaly changed by the addition of DBrBu or hexanedinitrile in $CHCl_3$ and exhibit its competitive guest stimuli-responsiveness. Furthermore, it is found that P5A-based host−guest chemistry and PE-based block copolymers are a perfect combination for the formation of stimuli-responsive polymeric materials. Thus, it is anticipated that this facile strategy may open up many new

opportunities for accessing a new class of polyolefin materials with structural diversity and functional utility.

Notes and references

1   A. J. Peacock, *Handbook of Polyethylene: Structures, Properties, and Applications*, Marcel Dekker, New York, USA 2000.
2   a) T. C. Chung, *Prog. Polym. Sci.*, 2002, **27**, 39; b) Y. Chen, L. Wang, H. Yu, Y. Zhao, R. Sun, G. Jing, J. Huang, H. Khalid, N. M. Abbasi, A. Muhammad, *Prog. Polym. Sci.*, 2015, **45**, 23.
3   a) F. Huang and H. W. Gibson, *Prog. Polym. Sci.*, 2005, **30**, 982; b) A. Harada, A. Hashidzume, H. Yamaguchi and Y. Takashima, *Chem. Rev.*, 2009, **109**, 5974; c) K. Karaky, C. Brochon, G. Schlatter and G. Hadziioannou, *Soft Matter*, 2008, **4**, 1165.
4   a) J. Araki and K. Ito, *Soft Matter*, 2007, **3**, 1456; b) F. Wang, C. Han, C. He, Q. Zhou, J. Zhang, C. Wang, N. Li and F. Huang, *J. Am. Chem. Soc.*, 2008, **130**, 11254; c) J. Zhan, Q. Li, Q. Hu, Q. Wu, C. Li, H. Qiu, M. Zhang and S. Yin, *Chem. Commun.*, 2014, **50**, 722; d) Y.-K. Tian, Y.-G. Shi, Z.-S. Yang and F. Wang, *Angew. Chem. Int. Ed.*, 2014, **53**, 6090; e) M. Arunachalam and H. W. Gibson, *Prog. Polym. Sci.*, 2014, **39**, 1043.
5   a) M. Zhang, D. Xu, X. Yan, J. Chen, S. Dong, B. Zheng and F. Huang, *Angew. Chem. Int. Ed.*, 2012, **51**, 7011; b) J. Zhan, M. Zhang, M. Zhou, B. Liu, D. Chen, Y. Liu, Q. Chen, H. Qiu and S. Yin, *Macromol. Rapid Commun.*, 2014, **35**, 1424.
6   a) X. Yan, D. Xu, X. Chi, J. Chen, S. Dong, X. Ding, Y. Yu and F. Huang, *Adv. Mater.*, 2012, **24**, 362; b) Y.-K. Tian and F. Wang, *Macromol. Rapid Commun.*, 2014, **35**, 337; c) P. Wei, X. Yan and F. Huang, *Chem. Soc. Rev.*, 2015, **44**, 815.
7   S. Li, G.-H. Weng, W. Lin, Z.-B. Sun, M. Zhou, B. Zhu, Y. Ye and J. Wu, *Polym. Chem.*, 2014, **5**, 3994.
8   X. Ji, S. Dong, P. Wei, D. Xia and F. Huang, *Adv. Mater.*, 2013, **25**, 5725.
9   a) R. G. Lopez, F. D'Agosto and C. Boisson, *Prog. Polym. Sci.*, 2007, **32**, 419; b) J. Z. Chen, K. Cui, S. Y. Zhang, P. Xie, Q. L. Zhao, J. Huang, L. P. Shi, G. Y. Li and Z. Ma, *Macromol. Rapid Commun.*, 2009, **30**, 532; c) J. Z. Chen, Q. L. Zhao, H. C. Lv, J. Huang, S. K. Cao and Z. Ma, *J. Polym. Sci. Part A: Polym. Chem.*, 2010, **48**, 1894; d) Y. Zhao, X. Shi, H. Gao, L. Zhang, F. Zhu, and Q. Wu, *J. Mater. Chem.*, 2012, **22**, 5737; e) Y. Zhao, H. Gao, G. Liang, F. Zhu and Q. Wu, *Polym. Chem.*, 2014 **5**, 962; f) H. Wang, C. Wu, G. Xia, Z. Ma, G. Mo and R. Song, *Soft matter*, 2015, **11**, 1778.
10   a) T. Ogoshi, H. Kayama, T. Aoki, T. Yamagishi, R. Ohashi and M. Mizuno, *Polym. J.*, 2014, **46**, 77; b) J. Li, A. Harada and M. Kamachi, *Bull. Chem. Soc. Jpn.*, 1994, **67**, 2808.
11   a) F. Wang, J. Zhang, X. Ding, S. Dong, M. Liu, B. Zheng, S. Li, L. Wu, Y. Yu, H. W. Gibson and F. Huang, *Angew. Chem. Int. Ed.*, 2010, **49**, 1090; b) P. Wei, J. Li, X. Yan and

Soft Matter Accepted Manuscript

Soft Matter Accepted Manuscript

Q. Zhou, *Org. Lett.*, 2014, **16**, 126; c) X.-Y. Hu, T. Xiao, C. Lin, F. Huang and L. Wang, *Acc. Chem. Res.*, 2014, **47**, 2041.

12 a) A. Harada, A. Hashidzume, H. Yamaguchi and Y. Takashima, *Chem. Rev.*, 2009, **109**, 5974; b) X. Liao, G. Chen, X. Liu, W. Chen, F. Chen and M. Jiang, *Angew. Chem. Int. Ed.*, 2010, **49**, 4409; c) K. L. Liu, Z. Zhang and J. Li, *Soft Matter*, 2011, **7**, 11290.

13 D.-S. Guo and Y. Liu, *Acc. Chem. Res.*, 2014, **47**, 1925.

14 a) Y. Liu, J. Shi, Y. Chen and C. F. Ke, *Angew. Chem. Int. Ed.*, 2008, **47**, 7293; b) A. E. Kaifer, *Acc. Chem. Res.*, 2014, **47**, 2160.

15 a) T. Ogoshi, Y. Nishida, T.-a. Yamagishi and Y. Nakamoto, *Macromolecules*, 2010, **43**, 3145; b) X.-Y. Hu, P. Zhang, X. Wu, W. Xia, T. Xiao, J. Jiang, C. Lin and L. Wang, *Polym. Chem.*, 2012, **3**, 3060; c) G. Yu, J. Zhou and X. Chi, *Macromol. Rapid Commun.*, 2015, **36**, 23; d) X. Chi, X. Ji, D. Xia and F. Huang, *J. Am. Chem. Soc.*, 2015, **137**, 1440.

16 a) T. Ogoshi, S. Kanai, S. Fujinami, T.-a. Yamagishi and Y. Nakamoto, *J. Am. Chem. Soc.*, 2008, **130**, 5022; b) D. Cao, Y. Kou, J. Liang, Z. Chen, L. Wang and H. Meier, *Angew. Chem. Int. Ed.*, 2009, **48**, 9721; c) M. Xue, Y. Yang, X. Chi, Z. Zhang and F. Huang, *Acc. Chem. Res.*, 2012, **45**, 1294; d) H. Chen, J. Fan, X. Hu, J. Ma, S. Wang, J. Li, Y. Yu, X. Jia and C. Li, *Chem. Sci.*, 2015, **6**, 197.

17 a) W. Si, L. Chen, X.-B. Hu, G. Tang, Z. Chen, J.-L. Hou and Z.-T. Li, *Angew. Chem. Int. Ed.*, 2011, **50**, 12564; b) Y. Yao, M. Xue, J. Chen, M. Zhang and F. Huang, *J. Am. Chem. Soc.*, 2012, **134**, 15712; c) C. Li, *Chem. Commun.*, 2014, **50**, 12420; d) X. Liao, L. Guo, J. Chang, S. Liu, M. Xie and G. Chen, *Macromol. Rapid Commun.*, 2015, DOI: 10.1002/marc.201500167.

18 a) Z. Zhang, B. Xia, C. Han, Y. Yu and F. Huang, *Org. Lett.*, 2010, **12**, 3285; b) Z. Zhang, Y. Luo, J. Chen, S. Dong, Y. Yu, Z. Ma and F. Huang, *Angew. Chem. Int. Ed.*, 2011, **50**, 1397.

19 a) J. Li, X. Ni, Z. Zhou and K. W. Leong, *J. Am. Chem. Soc.*, 2003, **125**, 1788; b) K. L. Liu, S. H. Goh and J. Li, *Macromolecules*, 2008, **41**, 6027.

20 a) C. Li, X. Shu, J. Li, S. Chen, K. Han, M. Xu, B. Hu, Y. Yu and X. Jia, *J. Org. Chem.*, 2011, **76**, 8458; b) C. Li, K. Han, J. Li, H. Zhang, J. Ma, X. Shu, Z. Chen, L. Weng and X. Jia, *Org. Lett.*, 2011, **14**, 42; c) X. Shu, J. Fan, J. Li, X. Wang, W. Chen, X. Jia and C. Li, *Org. Biomol. Chem.*, 2012, **10**, 3393; d) X. Shu, S. Chen, J. Li, Z. Chen, L. Weng, X. Jia and C. Li, *Chem. Commun.*, 2012, **48**, 2967.

21 a) A. Wang, J. Huang and Y. Yan, *Soft Matter*, 2014, **10**, 3362; b) L. Xu, L. Feng, Y. Han, Y. Jing, Z. Xian, Z, Liu, J. Huang and Y. Yan, *Soft Matter*, 2014, **10**, 4686; c) S. Liu, L. Zhao, Y. Yan and J. Huang, *Soft Matter*, 2015, **11**, 2752.